GSA Data Repository Item 2016164
Sinclair, H.D., Mudd, S.M., Dingle, E., Hobley, D.E.J., Robinson, R., and Walcott, R., 2016, Squeezing river catchments through tectonics: Shortening and erosion across the Indus Valley, NW Himalaya: GSA Bulletin, doi:10.1130/B31435.1.

OSL Analyses

SAMPLE PREPARATION

Samples were prepared using standard OSL procedures. Material was desiccated at 50 °C to enable calculation of water content, and then sieved to extract the 180–212 μm grain size fraction. Approximately 10 g of the 180–212 μm grain size fraction was treated with 30% HCl for 30 min to remove $CaCO_3$. Samples were agitated throughout the treatment, and once complete, HCl was replaced with 30% H_2O_2 to remove organic material. The duration of H_2O_2 treatment varied between samples, dependent upon the amount of organic material present, and two H_2O_2 treatments were necessary for some samples with a high organic content. Once effervescence ceased, the H_2O_2 was decanted, the sample was washed four times with deionised water and desiccated at 50 °C. Quartz is extracted from polymineral sediment residues through density separations using LST fastfloat (sodium heteropolytungstate dissolved in deionized water). Heavy minerals (>2.68 g cm^{-3}) were separated from the lighter fraction, and the target 2.58–2.68 gcm^{-3} fraction was further separated from the <2.58 g cm^{-3} material. The target fraction was washed five times with deionised water to ensure removal of all LST. Final separates were dried and etched with 40% HF for 40 min to remove any contaminating feldspar; all samples were agitated at 5 min intervals throughout treatment. The etched quartz was treated with 30% HCl for 30 min to remove any carbonates produced during HF etching.

LUMINESCENCE MEASUREMENTS

All analyses were carried out using either a TL-DA-15 or TL-DA-20 Risø reader, equipped with an EMI 9235QA photomultiplier and 7.5 mm Hoya U-340 filter. Blue (470 ± 20 nm) and infrared (~870 nm) diodes operated at 90% and 40% power, respectively, were used for stimulation and irradiation was achieved using a $^{90}Sr/^{90}Y$ beta source. Readers were calibrated using quartz prepared at the Risø National Laboratory in Denmark. Quartz was applied to stainless steel discs (10 mm Ø, 1 mm thick) using silicon grease and the aliquot size was regulated using a small (2 mm Ø, ~35 grain) mask.

Samples were analyzed using the single aliquot regenerative dose (SAR) protocol (Murray and Wintle, 2000). The equivalent dose (D_e) was calculated from measurements of the luminescence response following stimulation of the natural luminescence (L_n) and a series of different regenerative doses (L_x) (Table DR1). The L_n and L_x measurements are normalized by measurement of the luminescence response (T_x) to a constant test dose (T_D). The ratio L_x/T_x is used to compensate for sensitivity changes of the quartz throughout analysis and L_x/T_x measurements are used to obtain a range of values which bracket L_n/T_x, allowing D_e interpolation with minimal associated errors (Banerjee et al., 2000).

The sample is heated prior to making the luminescence measurements in order to reduce the contribution of luminescence from unstable trap, which cause erroneous dose determinations. The temperature of the pre-L_x pre-heat (PH1) and the pre-T_x pre-heat (PH2) must be empirically determined for each sample under analysis. This was achieved through analysis of 8 disks with a dose-recovery pre-heat plateau experiment (Murray and Wintle, 2003), using a range of PH1 and PH2 temperatures ranging from 150 – 220 °C. The influence of a hot-bleach at 280 °C was also investigated (Murray and Wintle, 2003) and used on any samples experiencing thermal transfer and recuperation.

The SAR protocol with a PH1 of 180 - 220 °C used on the samples is provided in Table DR1. Aliquot acceptance criteria used are (1) recycling ratios within 10% of unity; (2) signal intensities ^{3} 3 σ above background; (3) infrared (IR) depletion ratio within 20% of unity (Duller, 2003); (4) D_e uncertainty ≤ 20% and (5) recuperation within 10% of the normalized maximum dose. The acceptance thresholds are moderate - high for the samples reflecting a range of sensitivities for quartz in the samples. The total aliquots accepted for the samples therefore varies; >50 (6 samples), >40 (7 samples), >30 (13 samples) and between 15 and 30 aliquots (4 samples).

ENVIRONMENTAL DOSE RATE DETERMINATION

The environmental dose rates (D_r) were calculated for each sample from the unsieved portions of the original sample; concentrations of U, Th, K and Rb were measured directly using solution ICP-MS (Thermo X-Series), a cosmic-dose component after Prescott and Hutton (1994) and an internal alpha dose rate of 5% from the decay of U and Th after Sutton and Zimmerman (1978). External α-dose rates were ignored as the alpha irradiated portion of quartz grains was removed by etching. The conversion factors of Adamiec and Aitken (1998) and beta-particle attenuation factors after Mejdahl (1979) have been used. Sample water content was calculated following desiccation at 50 °C, and an uncertainty of 5% assumed. Table DR2 contains the dosimetry data for the OSL samples from the southwestern and northeastern margins of the Shyok Valley.

ANALYSIS OF RESULTS

Most samples are characterized by large overdispersion values (broad D_e distributions) which describe the spread in the data not accounted for by analytical uncertainties (Galbraith and Roberts, 2012). Samples with overdispersion, greater than 20%, are assumed to reflect heterogeneous bleaching before deposition and the D_e data were analyzed within Excel to calcualate overdispersion and statistical parameters that are used to model the appropriate burial age (D_b). We adopted the age model selection criteria of Arnold and Roberts (2009). Most samples are modeled using the three component minimum age model (MAM-3; Galbraith et al., 1999) and the RStudio Luminescence package (Kreutzer et al., 2013), and two samples are modeled with a central age model. The kernel density and radial plots are presented in Figure DR2A and DR2B for each sample and the dosmietry and D_e data are presented in Table DR2.

REFERENCES CITED

Adamiec, G., and Aitken, M.J., 1998, Dose-rate conversion factors: update: Ancient TL, v. 16, p. 37–46.

Arnold, L.J., and Roberts, R.G., 2009, Stochastic modelling of multi-grain equivalent dose (De) distributions: implications for OSL dating of sediment mixtures: Quaternary Geochronology, v. 4, p. 204–230, doi:10.1016/j.quageo.2008.12.001.

Banerjee, D., Botter-Jensen, L., and Murray, A.S., 2000, Retrospective dosimetry: estimation of the dose to quartz using the single-aliquot regenerative-dose protocol: Applied Radiation and Isotopes, v. 52, p. 831–844, doi:10.1016/S0969-8043(99)00247-X.

Duller, G.A.T., Bøtter-Jensen, L., and Murray, A.S., 2003, Combining infrared-and green-laser stimulation sources in single-grain luminescence measurements of feldspar and quartz: Radiation Measurements, v. 37(4), p. 543-550.

Galbraith, R.F., and Roberts, R.G., 2012, Statistical aspects of equivalent dose and error calculation and display in OSL dating: an overview and some recommendations: Quaternary Geochronology, v. 11, p. 1–27, doi:10.1016/j.quageo.2012.04.020.

Galbraith, R.F., Roberts, R.G., Laslett, G.M., Yoshida, H., and Olley, J.M., 1999, Optical dating of single and multiple grains of quartz from jinmium rock shelter, northern Australia, part 1, Experimental design and statistical models: Archaeometry, v. 41, p. 339–364, doi:10.1111/j.1475-4754.1999.tb00987.x.

Kreutzer, S., Schmidt, C., Fuchs, M.C., Dietze, M., Fischer, M., and Fuchs, M., 2013, Introducing an R package for luminescence dating analysis: Ancient TL, v. 30, p. 1–8.

Mejdahl, V., 1979, Thermoluminescence Dating: Beta-Dose Attenuation in Quartz Grains.

Murray, A.S., and Wintle, A.G., 2000, Luminescence dating of quartz using an improved single aliquot regenerative dose protocol: Radiation Measurements, v. 32, p. 57–73, doi:10.1016/S1350-4487(99)00253-X.

Murray, A.S., and Wintle, A.G., 2003, The single aliquot regenerative dose protocol: potential for improvements in reliability: Radiation Measurements, v. 37, p. 377–381, doi:10.1016/S1350-4487(03)00053-2.

Prescott, J.R., and Hutton, J.T., 1994, Cosmic ray contributions to dose rates for luminescence and ESR dating: Large depths and long-term time variations: Radiation Measurements, v. 23, p. 497–500, doi:10.1016/1350-4487(94)90086-8.

Sutton, S.R., and Zimmerman, D.W., 1978, Thermoluminescence dating: radioactivity in quartz: Archaeometry, v. 20, p. 67–69, doi:10.1111/j.1475-4754.1978.tb00214.x.

FIGURE CAPTIONS

Figure DR1. Sedimentary log through the T1 terrace fill at Spituk. Left hand column is thickness of beds in centimeters. Second column is bed number.

Figure DR2. Sedimentary log through the T2 terrace fill at Spitka which is on southwestern margin of the Indus Valley opposite Spituk. Grid Ref: 34.11683°, 77.51964.

Figure DR3. Location of Swath that generated the mean topographic values illustrated in Figure 8A.

Figure DR2A. Kernel density and radial plots for each OSL sample from the southwestern margin of Indus valley. These plots both present the D_e distributions and uncertainties and illustrate the spread in the data and how the minimum or central age modeled (Table DR1) maps onto the distributions. Sample name is provided at the top of the kernel density plot.

Figure DR2B. Kernel density and radial plots for each OSL sample from the northeastern margin of Shyok Valley.

Sinclair, H.D., Mudd, S.M., Dingle, E., Hobley, D.E.J., Robinson, R., and Walcott, R., 2016, Squeezing river catchments through tectonics: Shortening and erosion across the Indus Valley, NW Himalaya: GSA Bulletin, doi:10.1130/B31435.1.

TABLE DR1. AN EXAMPLE QUARTZ SAR PROTOCOL USED FOR THE LADAKH SAMPLES

Natural/Regenerative Dose	20, 50, 75, 100, 0, 10, 10 Gy
TL (PH1)	180 - 200˚C, 10 s, 5˚C/s
IRSL (final cycle only)	20˚C, 40 s, 5˚C/s
OSL	125˚C, 40 s, 5˚C/s, 90% power (*Lx*)
Test Dose	20 Gy
TL (PH2)	180˚C, 10 s, 5˚C/s
OSL	125˚C, 40 s, 5˚C/s, 90% (*Tx*)
TL (hot bleach)	280˚C, 40s, 5˚C/s, 90%

TABLE DR2. LOCATIONS OF DATED SAMPLES

Sample	Latitude (°N)	Longitude (°E)
Markha2011-01	34.11998	77.42213
Markha2011-02	34.11998	77.42213
Markha2011-05	34.11998	77.42213
Markha2011-06	34.12009	77.42102
Spituk2011-01	34.1309	77.52539
Dung2011-01	34.11691	77.51977
Dung2011-02	34.11691	77.51977
Dung2011-03	34.115	77.52248
Basgo2011-01	34.226	77.26396
Basgo2011-02	34.226	77.26396
Basgo2011-03	34.22578	77.267
Zansk2011-01	34.13588	77.27848
Zansk2011-02	34.13588	77.27848
Nimmu2011-01	34.20192	77.34215
Nimmu2011-02	34.20128	77.34131
Nimmu2011-03	34.18956	77.36797
Nimmu2011-04	34.18956	77.36797

GSA Data Repository Item 2016164
Sinclair, H.D., Mudd, S.M., Dingle, E., Hobley, D.E.J., Robinson, R., and Walcott, R., 2016, Squeezing river catchments through tectonics: Shortening and erosion across the Indus Valley, NW Himalaya: GSA Bulletin, doi:10.1130/B31435.1.

TABLE DR3 DOSIMETRY, EQUIVALENT DOSE (D_E) AND OSL AGE ESTIMATES LADAKH SAMPLES

Sample	U (ppm)	Error (ppm)	Th (ppm)	Error (ppm)	K (%)	Error (%)	Rb (ppm)	Error (ppm)	H_2O content	Cosmic ($mGya^{-1}$)	Error (10%)	Total Qtz ($mGya^{-1}$)	Error ($mGya^{-1}$)	N	De Gy	Error Gy	Age ka	Error ka	Age Model
Markha2011-1	1.479	0.044	7.87	0.236	1.499	0.045	70.88	7.088	0.5	0.036	0.004	1.541	0.047	56	54.88	3.85	35.60	2.73	MAM-3
Markha2011-2	1.801	0.054	9.252	0.278	1.662	0.050	86.46	8.646	0.6	0.036	0.004	1.638	0.047	59	119.60	6.98	73.01	4.76	MAM-3
Markha2011-5	1.596	0.048	7.109	0.213	1.287	0.039	70.53	7.053	0.4	0.036	0.004	1.501	0.049	36	59.98	7.55	39.97	5.19	MAM-3
Markha2011-6	1.814	0.054	6.839	0.205	0.906	0.027	51.77	5.177	0.1	0.037	0.004	1.483	0.066	20	114.52	16.53	77.22	11.67	MAM-3
Spituk2011-1	2.009	0.060	8.749	0.262	0.937	0.028	49.35	4.935	0.1	0.268	0.027	2.059	0.078	31	56.65	5.85	27.52	3.03	MAM-3
Dung2011-1	2.532	0.076	11.83	0.355	1.78	0.053	98.35	9.835	0.4	0.376	0.038	2.712	0.080	53	31.83	1.59	11.74	0.68	MAM-3
Dung2011-2	2.594	0.078	12.48	0.374	1.92	0.058	109.9	10.99	0.4	0.376	0.038	2.685	0.084	53	51.29	1.10	19.11	0.73	CAM
Dung2011-3	3.466	0.104	13.16	0.395	1.875	0.056	107.8	10.78	0.9	0.382	0.038	2.146	0.058	53	47.18	2.56	21.98	1.33	MAM-3
Basgo2011-1	1.64	0.049	10.68	0.320	2.489	0.075	101	10.1	0.6	0.360	0.036	2.345	0.074	39	44.75	7.96	19.08	3.45	MAM-3
Basgo2011-2	1.414	0.042	7.592	0.228	2.011	0.060	66	6.6	0.4	0.056	0.006	1.993	0.067	37	17.49	1.60	8.78	0.86	MAM-3
Basgo2011-3	0.778	0.023	4.5	0.135	2.086	0.063	66.88	6.688	0.4	0.056	0.006	1.794	0.063	25	38.87	1.87	21.66	1.29	CAM
Zansk2011-1	2.051	0.062	9.959	0.299	0.813	0.024	36.6	3.66	0.5	0.300	0.030	1.599	0.048	15	30.99	10.62	19.39	6.67	MAM-3
Zansk2011-2	1.173	0.035	5.356	0.161	1.144	0.034	45.17	4.517	0.4	0.300	0.030	1.513	0.051	35	59.50	18.80	39.32	12.49	MAM-3
Nimmu2011-1	1.504	0.045	5.518	0.166	1.159	0.035	50.25	5.025	0.3	0.054	0.005	1.448	0.050	16	41.65	5.67	28.76	4.04	MAM-3
Nimmu2011-2	1.586	0.048	9.454	0.284	1.263	0.038	55.01	5.501	0.3	0.054	0.005	1.740	0.059	34	32.40	3.09	18.62	1.88	MAM-3
Nimmu2011-3	1.831	0.055	7.82	0.235	0.813	0.024	52.3	5.23	0.1	0.282	0.028	1.870	0.071	45	23.88	1.53	12.77	0.95	MAM-3
Nimmu2011-4	2.142	0.064	8.464	0.254	0.982	0.029	53.79	5.379	0.1	0.282	0.028	2.123	0.081	55	24.28	1.70	11.44	0.91	MAM-3

Supplementary figure 1, Sinclair et al.

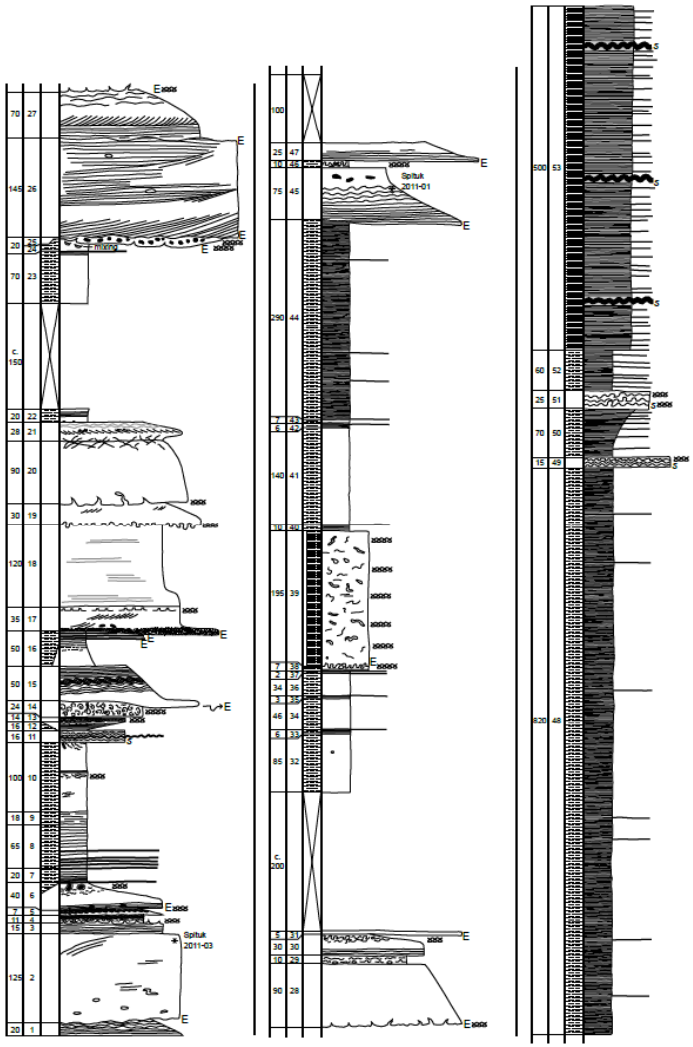

Supplementary figure 2, Sinclair et al.

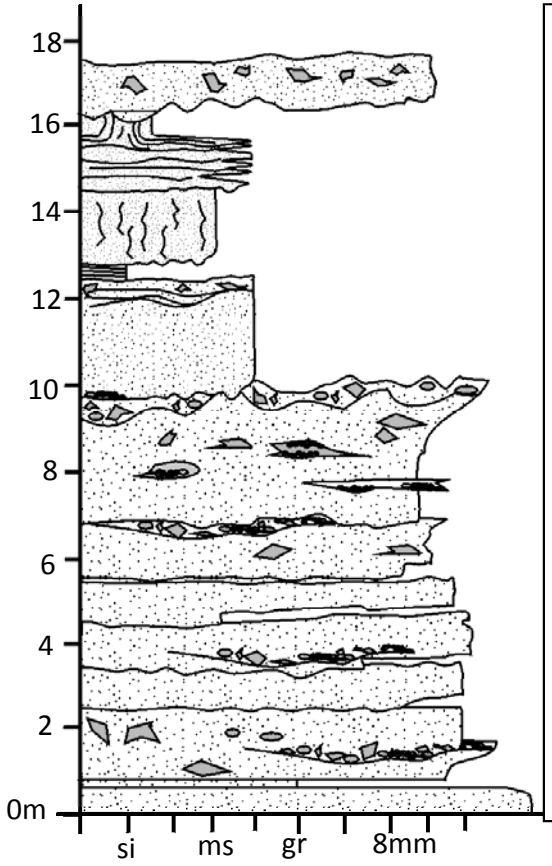

Poorly bedded gravels and breccias forming modern fan surface.	Modern alluvial fan
Planar bedded med/fine sandst., v. poorly sorted. Rootlets and shell fragments. Some carbonaceous layers.	Sand accumulation at margins of lake rich in vegetation
Planar laminated, cream-coloured silts and muds.	Seasonal fine sediment fall-out into lake
Unsorted coarse gravels with vague discontinuous bedding. Little matrix, muddy coating to clasts.	Debris flows and high concentration stream flows on alluvial fan

Supplementary figure 3, Sinclair et al.

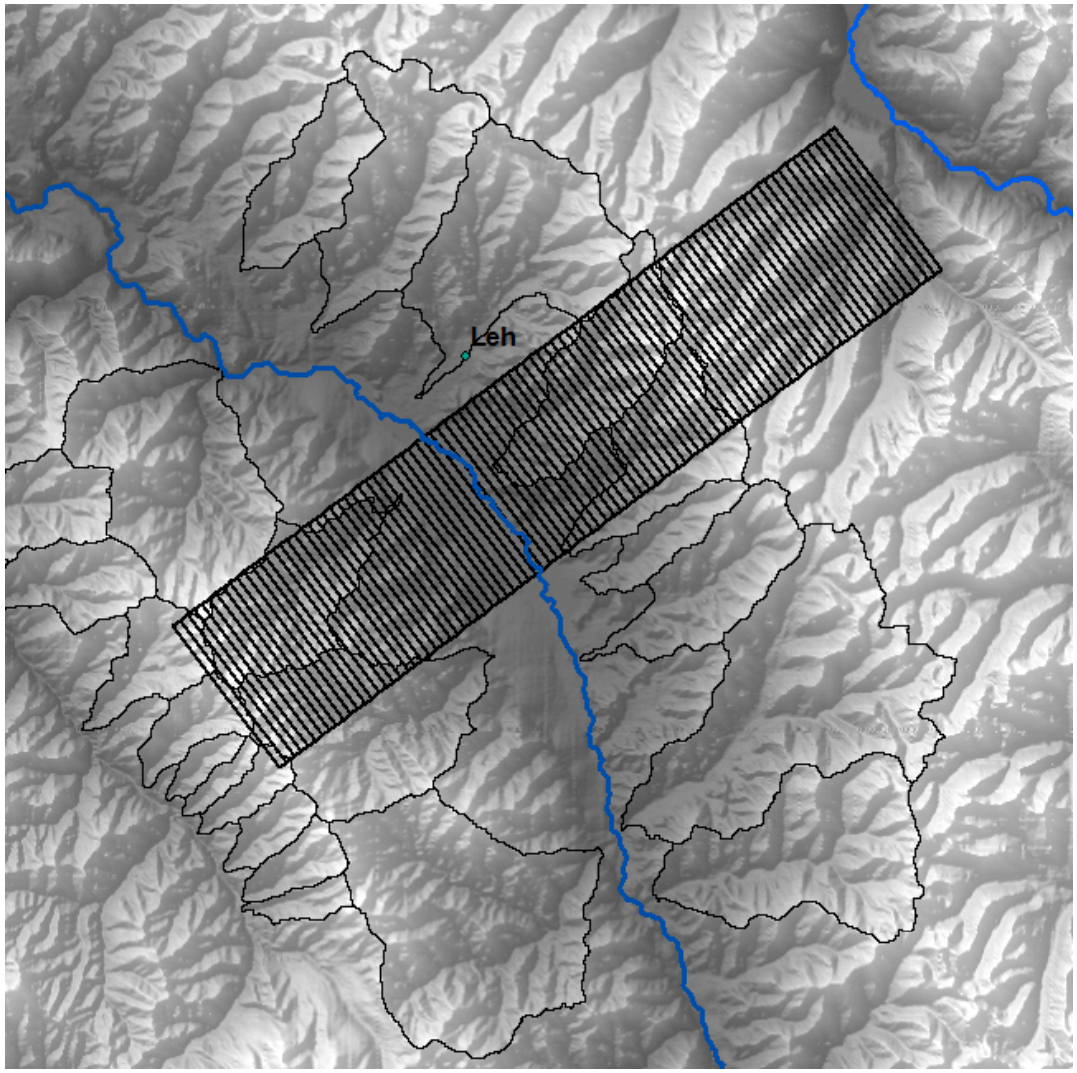

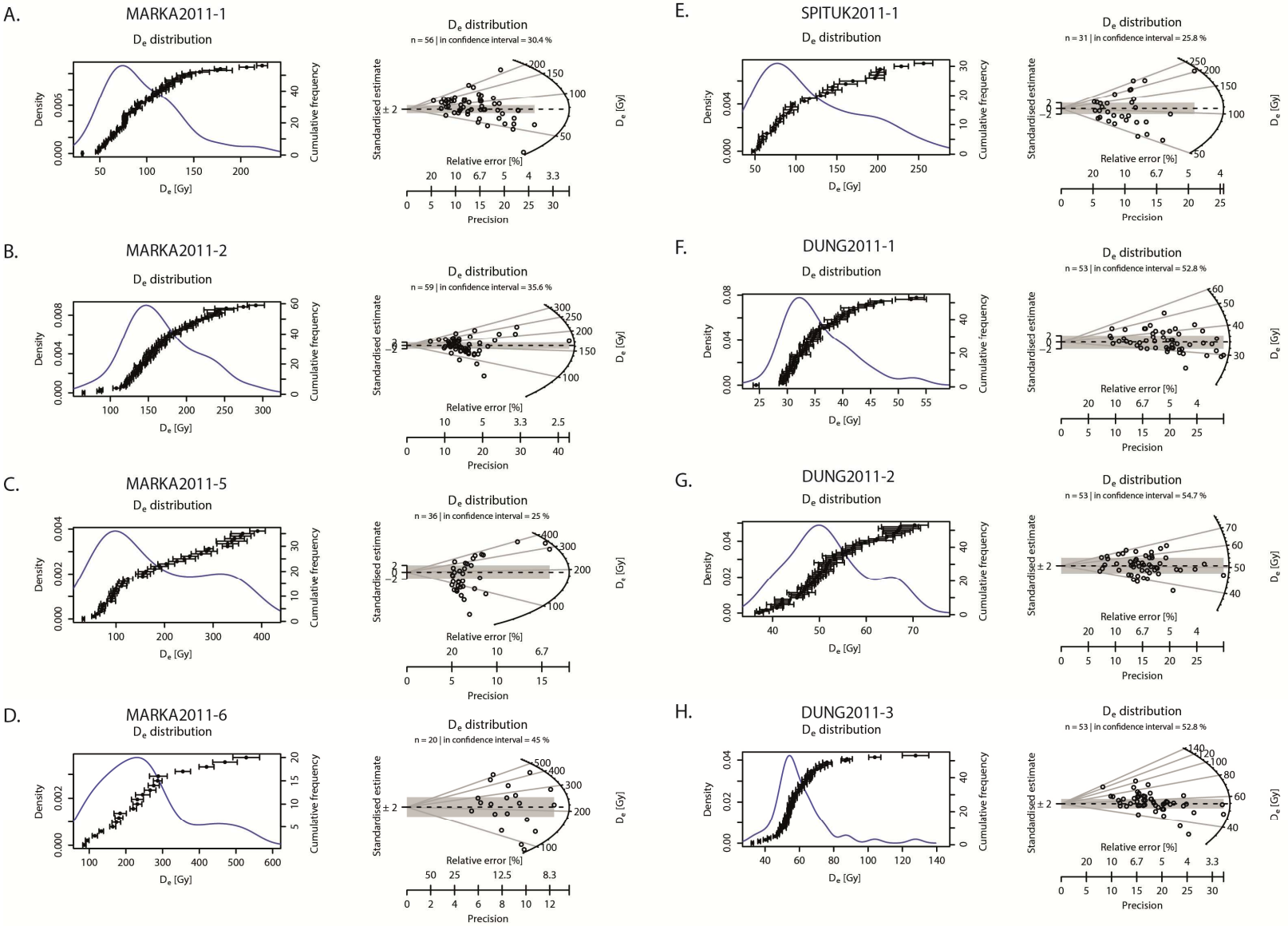
A.
MARKA2011-1
De distribution
n = 56 | in confidence interval = 30.4 %
B.
MARKA2011-2
De distribution
n = 59 | in confidence interval = 35.6 %
C.
MARKA2011-5
De distribution
n = 36 | in confidence interval = 25 %
D.
MARKA2011-6
De distribution
n = 20 | in confidence interval = 45 %
E.
SPITUK2011-1
De distribution
n = 31 | in confidence interval = 25.8 %
F.
DUNG2011-1
De distribution
n = 53 | in confidence interval = 52.8 %
G.
DUNG2011-2
De distribution
n = 53 | in confidence interval = 54.7 %
H.
DUNG2011-3
De distribution
n = 53 | in confidence interval = 52.8 %
Density
Cumulative frequency
De [Gy]
Standardised estimate
Relative error [%]
Precision

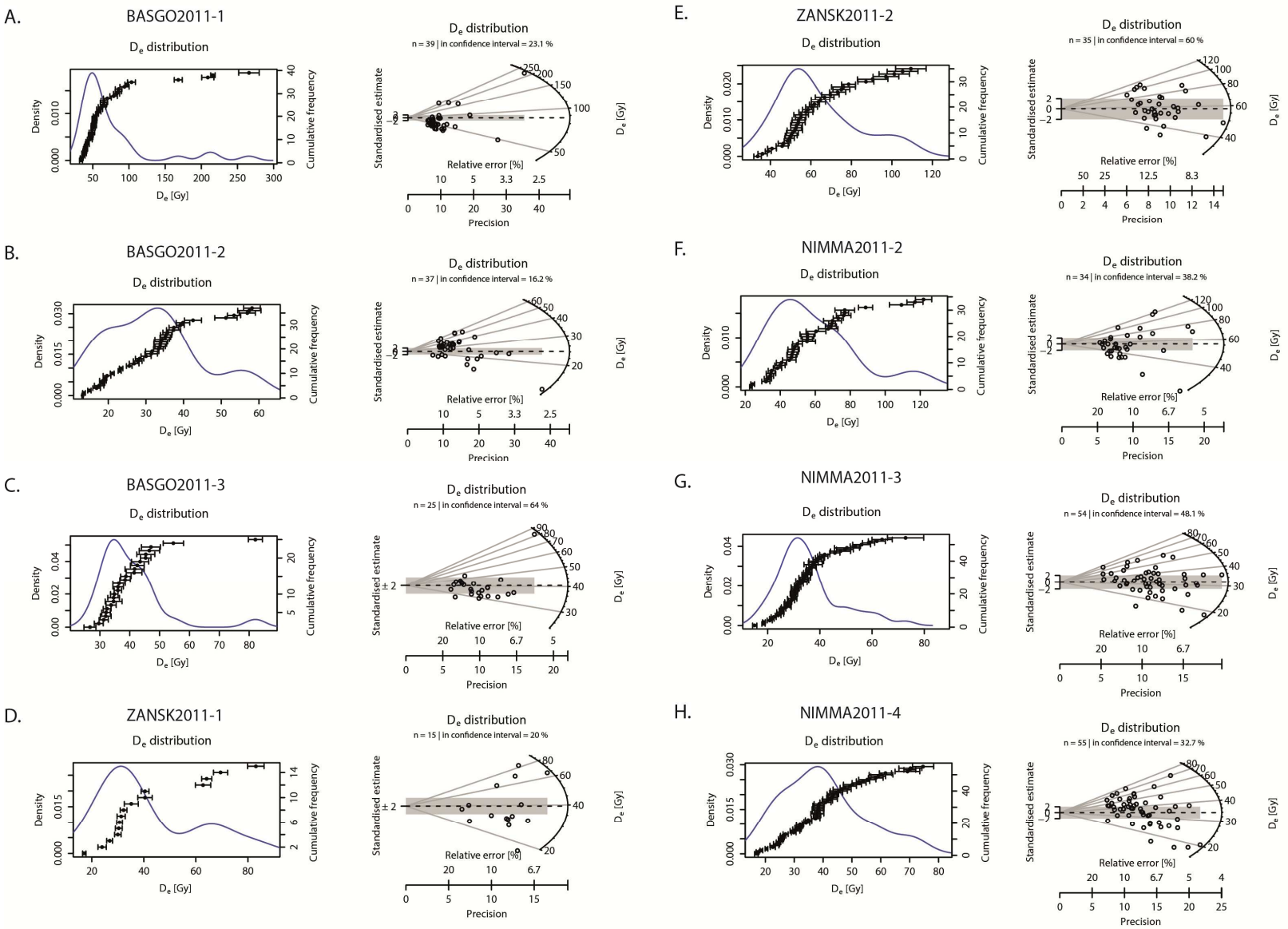
A.
BASGO2011-1
De distribution
n = 39 | in confidence interval = 23.1 %
B.
BASGO2011-2
De distribution
n = 37 | in confidence interval = 16.2 %
C.
BASGO2011-3
De distribution
n = 25 | in confidence interval = 64 %
D.
ZANSK2011-1
De distribution
n = 15 | in confidence interval = 20 %
E.
ZANSK2011-2
De distribution
n = 35 | in confidence interval = 60 %
F.
NIMMA2011-2
De distribution
n = 34 | in confidence interval = 38.2 %
G.
NIMMA2011-3
De distribution
n = 54 | in confidence interval = 48.1 %
H.
NIMMA2011-4
De distribution
n = 55 | in confidence interval = 32.7 %
Density
Cumulative frequency
De [Gy]
Standardised estimate
Relative error [%]
Precision